Computer Modeling in Engineering & Sciences

Tech Science Press

https://doi.org/10.32604/cmes.2026.078569

ARTICLE

Predicting Tropical Cyclone Genesis Location Using STAG-Net: A Spatio-Temporal Attention-Gated Network

Kalim Sattar[1], Malik Muhammad Saad Missen[2], Syeda Zoupash Zahra[1,3], Najia Saher[4], Rab Nawaz Bashir[3,5,6,*], Oumaima Saidani[7], Shahid Kamal[5] and Muhammad I. Khan[6]

[1]Department of Information Technology, The Islamia University of Bahawalpur, Bahawalpur, Pakistan
[2]Department of Software Engineering, The Islamia University of Bahawalpur, Bahawalpur, Pakistan
[3]Department of Computer Science, COMSATS University Islamabad, Vehari Campus, Vehari, Pakistan
[4]Department of Artificial Intelligence, The Islamia University of Bahawalpur, Bahawalpur, Pakistan
[5]Center for Advanced Analytics, CoE for Artificial Intelligence, Faculty of Computing and Informatics, Multimedia University, Cyberjaya, Selangor, Malaysia
[6]Artificial Intelligence and Data Analytics Laboratory (AIDA), College of Computer and Information Sciences (CCIS), Prince Sultan University, Riyadh, Saudi Arabia
[7]Department of Information Systems, College of Computer and Information Sciences, Princess Nourah bint Abdulrahman University, P.O. Box 84428, Riyadh, 11671, Saudi Arabia

*Corresponding Author: Rab Nawaz Bashir. Email: rabnawaz@cuivehari.edu.pk

Received: 04 January 2026; Accepted: 23 March 2026; Published: 27 May 2026

ABSTRACT: Tropical Cyclone (TC) genesis forecasting is an important aspect of early warning systems, as it allows the adoption of early warnings and mitigation plans. However, existing methods often rely on binary classification or fail to capture the complex spatio-temporal dependencies that govern TC formation. To address this limitation, this study introduces STAG-Net, a novel Spatio-Temporal Attention-Gated Network designed to directly predict the geographical coordinates of TC genesis. The model uses multivariate variables of meteorological factors such as u-wind, v-wind, relative humidity, temperature, and large-scale dynamic features using a Convolutional Neural Network (CNN), Gated Recurrent Units (GRUs), and a channel-wise attention mechanism in identifying both spatial and temporal characteristics. The methodology takes the initial tropical disturbance data as an input and obtains spatial features in the ERA5 reanalysis dataset that covers 37 isobaric pressure levels. The study also investigates the effect of grid resolution on prediction performance, as four grid sizes were compared, namely 10 × 10, 20 × 20, 30 × 30, and 40 × 40. The experimental results demonstrate that STAG-Net significantly outperforms existing baselines such as the Dynamic Spatio-temporal model (DST), Spatial Attention Fusing Network (Saf-Net), and a temporal-only model. Notably, the model achieves an average MAE of 2.67°, MSE of 13.24, RMSE of 3.45, and R^2 of 0.87045, corresponding to performance improvements of 9.75%, 26.25%, 12.92%, and 4.27%, respectively, over the baseline model. The results also indicate that the 30 × 30 grid configuration was found to be the most effective. The results highlight the significance of the proposed approach for the TC genesis location prediction task.

KEYWORDS: Tropical cyclone genesis; atmospheric dynamics; spatio-temporal analysis; deep learning; reanalysis data

1 Introduction

Tropical cyclone (TC) genesis forecasting is an important concern in atmospheric science and disaster risk management [1]. The term "cyclone genesis" is used to characterize the transition from a tropical disturbance to a tropical cyclone, as this is a critical phase that influences the storm's future trajectory and

development. It is imperative to ensure adequate forecasting of this phase at the earliest possible stage, as it provides significant lead time for proactive decision-making. This lead time can be effectively used to provide timely warnings and mobilise emergency response agencies in order to minimise potential socio-economic losses [2]. The importance of enhancing predictive capabilities is further underscored by the growth in the frequency and intensity of tropical cyclones, which may be worsened by the rising climate [3]. In numerous instances, conventional forecasting methodologies, which primarily rely on numerical weather prediction schemes [4] and heuristic warning criteria [5], are unable to identify weak or emerging disturbances that subsequently develop into strong cyclonic storms. This vulnerability is particularly evident in regions with sparse data or those located in low-latitude oceanic regions [6]. It is imperative to develop models that can leverage the extensive collection of climatic data and reveal the concealed forms associated with cyclogenesis. It would be beneficial to implement an alternative that is based on a data-driven approach to spatio-temporal atmospheric information and has the capacity to learn non-linear, multi-factorial relationships among the factors (pressure, temperature, wind, humidity, etc.). This field holds immense potential to transform cyclone early warning systems and improve climate resilience across vulnerable regions.

Traditional TC genesis prediction systems were based on both numerical weather prediction (NWP) [4] models and empirical indices [3] based on physical knowledge of atmospheric dynamics. Although these models have played an essential role in productive forecasting, they experience several limitations. Most pronouncedly, their coarse resolution fails to capture mesoscale structure and convective processes that are very crucial in the formation of cyclones. Furthermore, the traditional models require high computational power and have high forecasting error when lead times exceed 48 h [7]. In addition, often deterministic predictions do not provide the probabilistic meaning that is vital in risk-based decision-making. Even more sophisticated ensemble systems, like those applied in the S2S (Subseasonal to Seasonal) framework [8], do not perform well beyond a week's timeframe.

Statistical models [9–11] have also been employed for the TC genesis forecasting task. These models are conventionally based on empirical indices and regression methods using environmental data such as vorticity, wind shear, and humidity. Although these models are computationally effective, they fail to reflect non-linear interactions and capture spatio-temporal relationships, which restrict their effectiveness in predicting the location of TC genesis.

In the past few years, several researchers have utilized the effectiveness of machine learning for cyclone-genesis prediction. Studies [12,13] map TC genesis into a binary classification problem. These systems are effective in distinguishing non-developing tropical depressions from developing ones and enabling early warnings. The study [14] presents TC-Pred, a deep learning model based on the transformer, for predicting TC genesis using ERA5 spatiotemporal data. It takes advantage of long-range dependency learning achieved via attention mechanisms. The method performs better than the CNN and Convolutional Long Short-Term Memory (ConvLSTM) benchmarks. In the study [15], a spatiotemporal deep learning model is suggested using ConvLSTM to forecast the genesis of a tropical cyclone (TC) based on environmental fields from ERA5 data. It poses TC genesis prediction as a binary classification task of genesis vs. non-genesis-related events. Although the performance was good, the weaknesses are regional imbalance and less generalization across the basins.

Although in the recent past there have been significant improvements in the prediction of TC genesis using machine learning, current models have several major limitations, which highlight the need for further improvement. A prominent shortcoming is the overwhelming focus on binary classification, where models merely determine whether a disturbance will develop into a TC within a fixed lead time. Such models are indeed effective in the early detection but fail in the ability to give the absolute position of genesis, which is essential in targeted early alerts, resource placements, and activity scheduling. TC genesis models, such as

optimized Kalman Filter algorithm [12], TCGP-Net [15] use static or short-time temporal features to predict the genesis of occurrence at the current location of disturbance and do not consider the displacement of the disturbance location to a different spot within the field. Furthermore, the current TC genesis prediction studies do not focus much on the vertical structure of the atmosphere. In a majority of the reports, only a few isolated isobaric levels are assessed or averaged, disregarding the complete vertical structure that actually controls the cyclogenesis. It is possible that this simplification will cause the underrepresentation of features and lower model robustness. Thus, it becomes crucial to have a data-based model that allows prediction of the most likely genesis location while simultaneously studying all involved isobaric layers [16], offering a more spatially and vertically focused method of TC genesis forecasting.

To overcome these limitations, this study proposes a novel methodology for TC genesis location prediction. The proposed study utilizes ERA-5 reanalysis spatio-temporal data in grid format and predicts the coordinates of possible TC genesis. Pressure-level data for four different components (U-component of wind, V-component of wind, relative humidity, and temperature) across 37 different isobaric planes (1000 to 1 hPa) are extracted in four different grid sizes (10×10, 20×20, 30×30, and 40×40) based on the detected tropical disturbance at time t. The aim of the study is to predict the possible latitude and longitude ahead of time where it can intensify into a TC. The major contributions of this study are as follows:

- A novel methodology, Spatio-Temporal Attention-Gated Network (STAG-Net), is proposed for TC genesis location prediction by utilizing wide temporal information as well as deep atmospheric data in spatio-temporal format from ERA5 reanalysis.
- The impact of varying spatial grid sizes (10×10, 20×20, 30×30, and 40×40) is systematically evaluated to determine the optimal grid size for accurate TC genesis prediction.
- Conducted comprehensive experiments to analyze the contribution of four atmospheric components across 37 isobaric levels, identifying the most effective variable pair for enhancing prediction accuracy.

The rest of the study is organized as follows: Section 1.1 contains a survey of state-of-the-art research and its associated concerns. The methodology is described in Section 2. The evaluation of results is presented in Section 3. Lastly, Section 4 concludes the study by presenting the major findings and future directions.

1.1 Related Work

Predicting TC genesis falls into three broad categories, including numerical forecasting techniques, empirical indices, and data-driven techniques. Physical or ECMWF [17,18] and GFS numerical models [19] can be used to calculate atmospheric dynamics by solving physical equations, although they usually have high computing costs and initialization problems. Other empirical indices, such as the Genesis Potential Index (GPI) [3], measure multiple environmental variables through a past trend but are not dynamic to changing climate conditions. However, an alternative data-based approach, which involves machine learning models specifically, has gained prominence due to being able to learn complex spatio-temporal patterns in machine learning models in reanalysis data-based approaches with a higher level of accuracy and operational efficiencies of machine learning models.

1.1.1 Data-Driven Models

The statistical and machine learning models are a part of the data-driven models in predicting tropical cyclone genesis. The study by [20] used a statistical framework to determine important environmental factors of short-term TC genesis prediction. They have modeled the problem as a classification problem, where the validation was done using graphical model structure learning (PC algorithm) and logistic regression. However, the data imbalance and discretizations of statistical dependency are key limitations of statistical

models. The study [21] formulated a statistical-dynamical tropical cyclone genesis guidance tool based on global model outputs by carrying out a multiple logistic regression. The problem of genesis prediction was conceptualized in the study as a classification problem and found major predictors in basins. Even though the forecasts were traditionally well-calibrated, they had the drawbacks of the biases in models and the prediction imperfection of regional specificity.

Although these developments have occurred, there are complex nonlinear and spatio-temporal relationships that can hardly be represented using traditional statistical models. Therefore, more advanced machine learning-based models have been applied to improve tropical cyclone genesis prediction.

1.1.2 Machine Learning-Based Models

Machine learning-based methods have been used for meteorological tasks. The study [22] used an ensemble approach for TC path prediction. The study [23] used a ConvGRU model for TC intensity prediction up to 24 h.

The study [24] proposes a machine learning methodology to define the possibility of mesoscale convective systems (MCSs) developing into a TC. Positioned as a classification task, it utilized AdaBoost as the classification algorithm, achieving an F1-score of 97.2 with a 6-h lead time. A major contribution is the combination of environmental and MCS-specific predictors, which provides better prediction than conventional methods such as the Genesis Potential Index (GPI).

The study [25] proposes a machine learning framework for long-term TC genesis prediction using Support Vector Machine (SVM) and AdaBoost algorithms. By accounting for five important meteorological factors, the model successfully maps input features to genesis outcomes as a classification task. It balances the data and training splits and provides better spatio-temporal precision and generalization.

The study [26] uses multiple environmental variables to forecast TC genesis with a Maximum Entropy (MaxEnt) machine learning model. The model, trained on reanalysis data and tested on historical observations, provides more spatially accurate potential genesis index values compared to conventional genesis indices. When applied to CMIP6 future climate scenarios, it demonstrates a statistically significant reduction in TC genesis prediction error, indicating a complex nonlinear correlation between potential intensity and TC genesis.

The study [27] put forward a multiscale regression model to predict the frequency of TC genesis (TCGF) in the Northern Hemisphere. The model represents variability of observed TCGF in 1960–2019 in six climate-related predictors at interannual, interdecadal, and global warming time scales. Together with CMIP6 climate data, it forecasts basin-scale climate change in the near future, which gives a hybrid statistical-dynamical model that has a better decadal predictivity than longer-range historical trajectory-based prediction methods.

The study [28] proposes a novel methodology that combines CNN and Long Short-Term Memory (LSTM) within a deep learning framework to predict typhoons. It combines 3D and 2D CNNs to get spatial information based on atmospheric and ocean surface data, and LSTM acquires time-dependent information. The model is assessed using three regional datasets, and it is found to be better than the conventional numerical, statistical, and machine learning approaches, and this offers an innovative spatio-temporal reservoir-based technique to typhoon prediction, disaster warning, and preparedness.

The study [29] introduces a deep learning model, TCGNet, that combines Convolutional Neural Networks (CNNs) with channel- and spatial-attention mechanisms to emulate tropical cyclone genesis (TCG) under climate change conditions. Based on two historical and CMIP6 datasets, TCGNet shows improved prediction ability and generalization ability compared to the conventional statistical models.

It eliminates the need for manual feature selection, captures complex, spatio-temporal patterns in the environment, and extrapolates the lower frequency of TCG in the case of increased carbon emissions.

The study [15] establishes an enhanced spatiotemporal deep learning model, TC-Pred, in which TC intensity is predicted at high resolution. The most important contribution is a feature aggregation mechanism for multi-source environmental data and the incorporation of a convolutional transformer module into the sequence-to-sequence architecture to reduce sequential dependency problems. The task is positioned as a regression task by forecasting future TC intensities. The model uses the ConvGRU algorithm embedded within a deep neural network.

The study [30] leverage artificial intelligence to increase the predictability of extreme events on subseasonal to decadal timescales through the hybrid integration of artificial intelligence and climate models, along with best practices for robustness and interpretability.

The study [31] has proposed the XAI-GPI framework, which uses the combination of clustering, ensemble feature selection, and Shapley Additive Explanations (SHAP) to better estimate the genesis of tropical cyclones while providing transparent driver attribution. The study [32] suggests NeuralGCM, an ML-physics model to make efficient seasonal predictions of tropical cyclone activity with competitive performance. The study [33], the researchers suggest the use of uncertainty-sensitive cyclone forecasting using interpretability-driven white-box models, including decision trees and Bayesian rule lists.

Although the accuracy of tropical cyclone genesis prediction has been improved significantly with statistical and machine learning-based models, as shown in Table 1, they still have significant shortcomings. Most importantly, these models are binary classification models and do not directly predict TC genesis location. Additionally, these studies use a fixed grid size and fail to consider the best grid size. These gaps point to the need for a spatio-temporal modeling framework for predicting genesis coordinates as well as testing various grid sizes to identify a new grid size.

Table 1: Summary of machine learning-based approaches in TC prediction.

Study	Key Work	Technique Used	Limitation
[22]	Ensemble approach for TC path prediction	Ensemble learning	Did not incorporate deep spatio-temporal atmospheric data.
[23]	TC intensity prediction up to 24 h	ConvGRU	Focused only on short-term intensity; lacked wide temporal and spatial feature integration for genesis.
[24]	Classified MCSs likely to develop into TCs	AdaBoost	Relied on limited predictors; no evaluation of multi-level atmospheric variables or spatio-temporal data.
[25]	Long-term TC genesis prediction using five meteorological factors	SVM, AdaBoost	Focused only on binary classification of TC genesis without predicting the exact genesis location.

(Continued)

Table 1 (continued)

Study	Key Work	Technique Used	Limitation
[26]	Used MaxEnt for TC genesis potential under CMIP6 scenarios	Maximum Entropy (MaxEnt)	Improved over traditional indices but did not explore deep neural methods or spatial grid resolution sensitivity.
[27]	Multiscale regression for TCGF (1960–2019)	Statistical regression with climate predictors	Addressed frequency trends but not fine-grained spatio-temporal prediction of genesis events.
[28]	Hybrid CNN–LSTM for typhoon prediction with spatio-temporal features	CNN (2D/3D) + LSTM	Focused on intensity/path; did not systematically evaluate optimal spatial grid size or variable contributions.
[29]	TCGNet with CNN and attention for climate-driven genesis	CNN + Attention mechanisms	Strong spatio-temporal capacity but did not analyze multi-variable combinations across pressure levels.
[15]	TC-Pred with ConvGRU + convolutional transformer for intensity	ConvGRU + Transformer	Targeted intensity forecasting; sequential dependency issues remain, and no detailed variable-level analysis was conducted.

2 Proposed Methodology

This section describes the proposed methodology, which can be divided into two phases: feature construction and model development. The feature construction phase is based on data extraction and feature engineering to generate spatio-temporal data. Afterwards, the model development phase makes use of these features to train a predictive model that can effectively predict the location of TC genesis.

2.1 Problem Statement

In this study, TC genesis location prediction is formulated as a regression problem based on spatio-temporal data. Let T_b represent a detected tropical disturbance (tropical blob) at time t with an initial central location $loc_t = (lat_t, lon_t)$. The aim is to predict the future possible location $\hat{loc}_{t+n} = (\hat{lat}_{t+n}, \hat{lon}_{t+n})$ for TC genesis at time $t + n$, where $n \in \mathbb{N}$ denotes the lead time.

Let $\mathcal{X}_t \in \mathbb{R}^{g\times g\times v\times p}$ denote the spatio-temporal features extracted around T_b, where:

- $g \times g$ is the spatial grid size centered on T_b.
- v represents the number of atmospheric variables.
- p is the number of isobaric planes for pressure-level data.

The goal is to learn a regression function, as shown in Eq. (1):

$$f : \mathcal{X}_t \rightarrow \hat{\text{loc}}_{t+n} = (\hat{\text{lat}}, \hat{\text{lon}}) \tag{1}$$

that maps the input spatio-temporal features to the predicted genesis coordinates.

2.2 Feature Construction

The feature construction stage starts with the temporal identification of tropical disturbances, followed by the extraction of the spatio-temporal representation around each disturbance to be used in predictive modeling.

2.2.1 Step 1: Tropical Disturbance Identification

Let

$$\mathcal{D}_{\text{CMA}} = \{(t_i, lat_i, lon_i)\}_{i=1}^{N}$$

denote the CMA Best Track dataset [34], where each record captures the timestamp t_i and coordinates (lat_i, lon_i) of observed TCs, and the statistics of the refined CMA data are shown in Table 2. We define a tropical disturbance ${T_b}^i$ as the initial record for each developing system with a classification status below the tropical depression threshold, as shown in Eq. (2).

$$T_b^i = (t_i, lat_i, lon_i), \quad T_b^i \in \{\text{Disturbance}, \text{Low}\} \tag{2}$$

These ${T_b}^i$ are used to extract temporal features, as shown in Eq. (3), and serve as anchors for subsequent spatio-temporal feature extraction.

$$\mathbf{w}_i = \mathbf{w}_i^{(T)} \in \mathbb{R}^{T \times d_w} \tag{3}$$

where T represents time, and d_w represents the temporal features.

Table 2: Summary of dataset statistics for the selected tropical cyclone records from CMA data.

Dataset Attribute	Value
Targeted Basin	Northwest Pacific (WNP) Basin
Total Disturbance Samples	850
Training Samples	680
Testing Samples	170
Train-Test Split Ratio	80:20
Years Covered	1949–2017

2.2.2 Step 2: Spatial Grid Definition

For each detected disturbance, ${T_b}^i$, a square grid of size $g \times g$ (e.g., $10 \times 10, 15 \times 15, 30 \times 30, 40 \times 40$) is defined around its center (lat_i, lon_i). Let the grid be denoted as in Eq. (4):

$$\mathcal{G}_i = \left\{ (lat_i + \Delta y_m,\ lon_i + \Delta x_n) \,\middle|\, m, n \in \left[-\frac{g}{2}, \frac{g}{2}\right] \right\} \tag{4}$$

where Δy_m and Δx_n are the spatial steps in latitude and longitude, respectively.

2.2.3 Step 3: Multivariable, Multi-Level Atmospheric Data Extraction

From the ERA5 reanalysis dataset [35], we extract multiple variables (e.g., zonal wind u, meridional wind v, temperature T, and relative humidity RH) across multiple pressure levels $P = \{p_1, p_2, \ldots, p_{37}\}$ at time t_i.

These four variables were chosen because they are representative of the basic dynamical and thermodynamical processes that control TC genesis prediction. Previous studies have unanimously found mid-level vorticity, wind structure, temperature stratification, and moisture availability to be dominant predictors of genesis [12]. Moreover, some key indices, such as vertical wind shear, tilting, and moisture convergence, can be diagnostically established from u, v, T, and RH fields, which guarantees the physical completeness of the representation without redundancy.

For each variable v_k and pressure level p_j, as defined in Eq. (5):

$$x_{ijk} = v_k(\mathcal{G}_i, p_j, t_i) \tag{5}$$

This yields a 4D feature tensor for each sample i, as shown in Eq. (6):

$$\mathcal{X}_i = [x_{ijk}] \in \mathbb{R}^{g\times g\times v\times p} \tag{6}$$

where:

- $g \times g$ is the spatial resolution.
- $v = 4$ is the number of variables.
- $p = 37$ is the number of isobaric pressure levels.

Each tensor $\mathcal{X}_i$ captures the spatial, vertical, and variable-wise atmospheric snapshot centered on the tropical disturbance at time t_i, as shown in Fig. 1.

2.2.4 Step 4: Single-Level Atmospheric Data Extraction

Sea surface temperature (SST) is extracted from the ERA5 single-level reanalysis dataset as a surface variable without vertical pressure dependence. Unlike multi-level atmospheric variables defined across pressure levels $P = \{p_1, \ldots, p_{37}\}$, SST is defined only at the surface level ($p = 0$).

For each tropical cyclone instance at time t_i and center (ϕ_i, λ_i), a spatial grid of size $G \times G$ (with $G = 3$ in this study) is constructed as follows:

$$\mathrm{SST}_i(m, n) = \mathrm{SST}(t_i, \phi_i + \Delta\phi_m, \lambda_i + \Delta\lambda_n), \quad m, n \in \{1, \ldots, G\} \tag{7}$$

The resulting spatial tensor is represented as:

$$\mathbf{X}_i^{\mathrm{SST}} \in \mathbb{R}^{1\times G\times G} \tag{8}$$

To integrate SST into the temporal branch, the spatial grid is vectorized and concatenated with the temporal feature representation:

$$\mathbf{w}_i \in \mathbb{R}^{T\times d_w} \quad \Rightarrow \quad \tilde{\mathbf{w}}_i \in \mathbb{R}^{T\times (d_w+G^2)} \tag{9}$$

where T denotes the temporal length, and d_w represents the original temporal feature dimension.

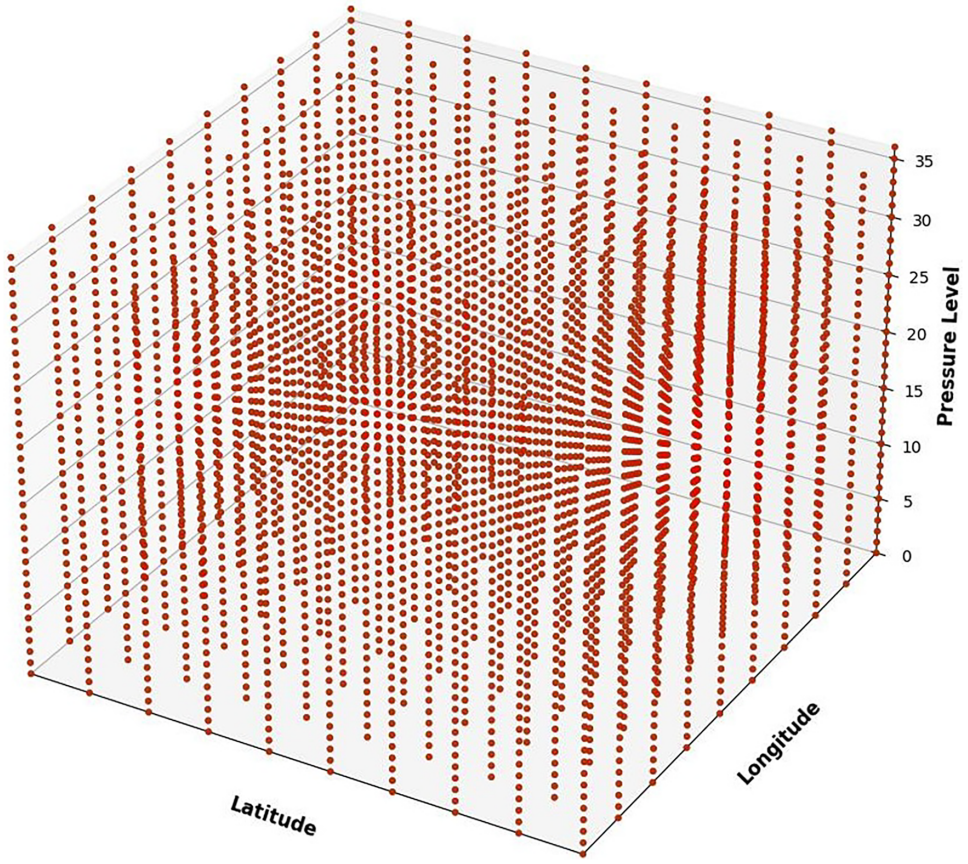

Figure 1: Representation of spatio-temporal feature extraction for a single atmospheric component.

2.3 Proposed Model

The proposed STAG-Net (Spatio-Temporal Attention-Gated Network) predicts the TC genesis location by utilizing wide temporal information as well as deep atmospheric data in spatio-temporal format, as shown in Fig. 2. The proposed model is a hybrid network structure composed of a gated recurrent unit (GRU) for sequential temporal learning in the ground-level features of tropical disturbances and multi-channel CNNs with channel-wise attention for extracting rich representations from the 4D atmospheric features. STAG-Net also adds GRU-based temporal encoding over pressure levels to capture vertical dynamics. The model achieves its prediction goal by combining wide and deep feature representations using a fully connected fusion layer, which produces the predicted coordinates for the potential TC genesis area.

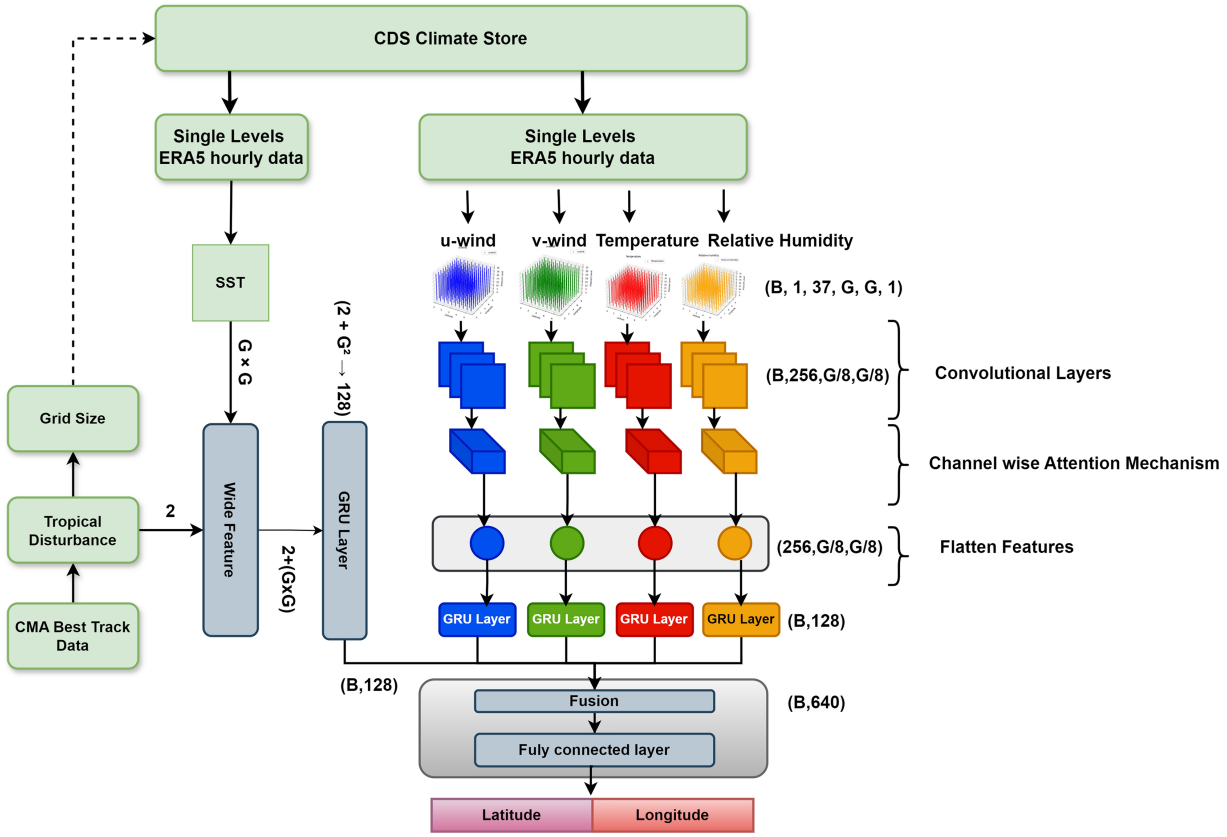

Figure 2: Proposed STAG-Net model for TC genesis location prediction.

2.3.1 Temporal Encoding via GRU

We use a two-layer GRU to process the temporally wide input as in Eq. (10):

$$\begin{aligned} \mathbf{h}_t^{(1)} &= \mathrm{GRU}^{(1)}(\mathbf{w}_i) \in \mathbb{R}^{T\times H_1}, \\ \mathbf{h}_t^{(2)} &= \mathrm{GRU}^{(2)}(\mathbf{h}_t^{(1)}) \in \mathbb{R}^{T\times H_2} \end{aligned} \tag{10}$$

where w_i describes the temporal features at time T, $h_t^{(1)}$ represents the intermediate hidden feature for the GRU layer, and $h_t^{(2)}$ represents the deeper temporal representation after a second GRU layer. Final wide feature can be defined as in Eq. (11):

$$\mathbf{f}_w = \mathbf{h}_T^{(2)} \in \mathbb{R}^{H_2} \tag{11}$$

2.3.2 Spatial Feature Encoding via CNN

Each variable X_i at time step t is a 3D tensor of shape $[C, H, W]$ and is passed through three convolutional blocks with channel-wise attention.

Convolutional Block: The initial input to the convolutional pipeline is denoted as $z^{(0)} = \mathcal{X}_i^{(v)}[:,:,:]$, where $\mathcal{X}_i = [x_i{}^{(v)}] \in \mathbb{R}^{g\times g\times p}$ represents the spatial grid for the vth atmospheric variable across $g \times g$ latitude-longitude cells and p pressure levels for the ith sample. The colon operator indicates that all spatial and vertical dimensions are included. This tensor is then passed through multiple convolutional layers.

At the lth layer, the output feature map $\mathbf{z}^{(l)}$ is computed as $\mathbf{z}^{(l)} = \mathrm{ReLU}(\mathrm{Conv}^{(l)}(\mathbf{z}^{(l-1)}))$, where $\mathrm{Conv}^{(l)}$ denotes a 2D convolution operation applied with a learnable kernel, and ReLU is the Rectified Linear Unit activation function, as shown in Eq. (12). This non-linearity introduces the ability to learn complex spatial representations.

$$\mathbf{z}^{(l)} = \mathrm{ReLU}(\mathrm{Conv}^{(l)}(\mathbf{z}^{(l-1)})), \quad \mathbf{z}^{(0)} = \mathcal{X}_i^{(v)}[:,:,:] \tag{12}$$

Channel-Wise Attention: At each block, attention is applied as in Eq. (13). The attention map $A^{(l)}$ is computed by applying a 1×1 convolution followed by a sigmoid activation σ on the feature map $z^{(l)}$. The output feature $z^{(l)}$ is then scaled element-wise using $\odot$ with the attention map.

$$\mathcal{A}^{(l)} = \sigma(\mathrm{Conv}_{1\times1}(\mathbf{z}^{(l)})), \quad \mathbf{z}^{(l)} = \mathbf{z}^{(l)} \odot \mathcal{A}^{(l)} \tag{13}$$

After 3 layers of Conv-Attention-Pooling, the spatial feature is flattened as in Eqs. (14) and (15):

$$\mathbf{f}_t^{(v)} = \mathrm{FC}(\mathrm{Flatten}(\mathbf{z}^{(3)})) \in \mathbb{R}^{H_c} \tag{14}$$

The CNN-encoded features for each variable across T are:

$$\left\{\mathbf{f}_1^{(v)}, \mathbf{f}_2^{(v)}, \ldots, \mathbf{f}_T^{(v)}\right\} \in \mathbb{R}^{T\times H_c} \tag{15}$$

Eq. (16) represents the use of a Gated Recurrent Unit (GRU) to process a sequence of feature vectors $[\mathbf{f}_1^{(v)}, \ldots, \mathbf{f}_T^{(v)}]$ for each variable v. The GRU captures temporal dependencies across the sequence and outputs hidden states $h_t^{(v)}$ that are further utilized for the final feature vector $\mathbf{f}_n$, as shown in Eq. (17).

$$\mathbf{h}_t^{(v)} = \mathrm{GRU}^{(v)}\left([\mathbf{f}_1^{(v)}, \ldots, \mathbf{f}_T^{(v)}]\right) \in \mathbb{R}^{T\times H_v} \tag{16}$$

$$\mathbf{f}_n = \mathbf{h}_T^{(v)} \in \mathbb{R}^{H_v} \tag{17}$$

2.3.3 Feature Fusion and Output Layer

We concatenate the wide and deep features from each variable as in Eq. (18):

$$\mathbf{f}_{\mathrm{concat}} = [\mathbf{f}_w, \mathbf{f}_{u_i}, \mathbf{f}_v, \mathbf{f}_t, \mathbf{f}_r] \in \mathbb{R}^{H_2+4H_v} \tag{18}$$

This vector is passed through two dense layers as in Eqs. (19) and (20):

$$\mathbf{z} = \mathrm{ReLU}(\mathbf{W}_1\mathbf{f}_{\mathrm{concat}} + \mathbf{b}_1) \in \mathbb{R}^{64} \tag{19}$$

$$\hat{y}_i = \mathbf{W}_2\mathbf{z} + \mathbf{b}_2 \in \mathbb{R} \tag{20}$$

where y_i is the predicted location of the TC genesis.

The model is trained using Mean Absolute Error (L1 loss) as in Eq. (21).

$$\mathcal{L} = \frac{1}{N}\sum_{i=1}^{N}|\hat{y}_i - y_i| \tag{21}$$

3 Experimental Evaluation

To assess the effectiveness of the proposed STAG-Net framework in predicting the location of TC genesis, a comprehensive set of experiments was carried out using spatio-temporal features based on ERA5

reanalysis data. The analysis aims to determine the effectiveness of the model in its capability to determine TC genesis coordinates ahead of time, given the initial tropical disturbance data.

3.1 Hyperparameter Setting

The chosen hyperparameters represent an optimized training scheme of the STAG-Net model, as shown in Table 3. We use Adam optimizer because it is good at dealing with sparse gradients and a learning rate of 0.0007 to get stable convergence. The model is based on L1 Loss (MAE) to emphasize the avoidance of large errors. The model is trained for 128 epochs with 128 batch sizes, which is a trade-off between computational performance and learning stability. The data is split as 80:20 in terms of training and testing. The architectural building block consists of three convolutional layers containing a gradually increasing number of channels (64, 128, 256), Max Pooling for spatial down-sampling and attention layers that increase the discriminative power of the features after each convolution stage.

Table 3: Hyperparameter settings for the proposed STAG-Net model.

Hyperparameter	Value/Setting
Optimizer	Adam
Learning rate (lr)	0.0007
Loss function	L1 Loss (Mean Absolute Error)
Epochs	128
Batch size	128
Train–test split	80:20 ratio
CNN layers	3 convolutional layers
CNN channels	64 → 128 → 256
Attention layers	3 (one after each conv layer)
Pooling	Max pooling (2 × 2)

3.2 Evaluation Metrics

Evaluation metrics used in this study are defined as in Eqs. (22)–(24).

$$\text{MAE} = \frac{1}{n}\sum_{i=1}^{n}|y_i - \hat{y}_i| \tag{22}$$

$$\text{RMSE} = \sqrt{\frac{1}{n}\sum_{i=1}^{n}(y_i - \hat{y}_i)^2} \tag{23}$$

$$R^2 = 1 - \frac{RSS}{TSS} \tag{24}$$

where:

- n defines the total number of samples.
- y_i represents the actual coordinates.
- $\hat{y}_i$ represents the predicted coordinates.
- RSS represents the residual sum of squares.
- TSS is the total sum of squares.

3.3 Results

3.3.1 Performance of Proposed Model

The performance of the proposed model, as shown in Table 4, indicates clear evidence that the proposed model ((u, v, r, t, wide) + attention) demonstrates strong predictive capability for TC genesis locations. Particularly, it has the lowest MAE for latitude (1.7995°) and longitude (3.5566°). The results indicate minimal error between predicted and actual genesis coordinates. The model achieved R^2 values (0.8399 and 0.901 for latitude and longitude, respectively), implying that it explains more than 84% of latitudinal variation and almost 90% of longitudinal variation, as shown in Fig. 3. Results indicate that component-wise fusion plays an important role in model performance. Wide features capture temporal dynamics, while the deep CNN layers extract spatial patterns from multi-channel reanalysis variables (u, v, r, t). The combination of both temporal and spatial patterns achieves the lowest MAE. The fusion network enhances the capability of the model by learning complex spatio-temporal patterns for TC genesis location prediction.

Table 4: Performance comparison of component-wise fusion in the STAG-Net model.

Model	Latitude				Longitude			
	MAE	MSE	RMSE	R^2	MAE	MSE	RMSE	R^2
u, wide	2.0745	7.2062	2.6844	0.7807	4.0045	26.6377	5.1612	0.8757
u, v, wide	1.8591	5.9616	2.4416	0.8186	4.4712	32.8530	5.7318	0.8467
u, v, r, wide	1.8614	5.3833	2.3202	0.8362	4.0529	28.3969	5.3289	0.8675
u, v, r, t	2.2033	8.2199	2.8670	0.7498	7.2366	79.3061	8.9054	0.6299
u, v, r, t, wide (without SST)	1.9902	6.4183	2.5334	0.8047	4.0082	26.0072	5.0997	0.8786
u, v, r, t, wide (with SST)	1.8726	5.9821	2.4458	0.8243	3.9145	24.7684	4.9767	0.8841
u, v, r, t, wide, attention	1.7995	5.2590	2.2932	0.8399	3.5566	21.2238	4.6069	0.9010

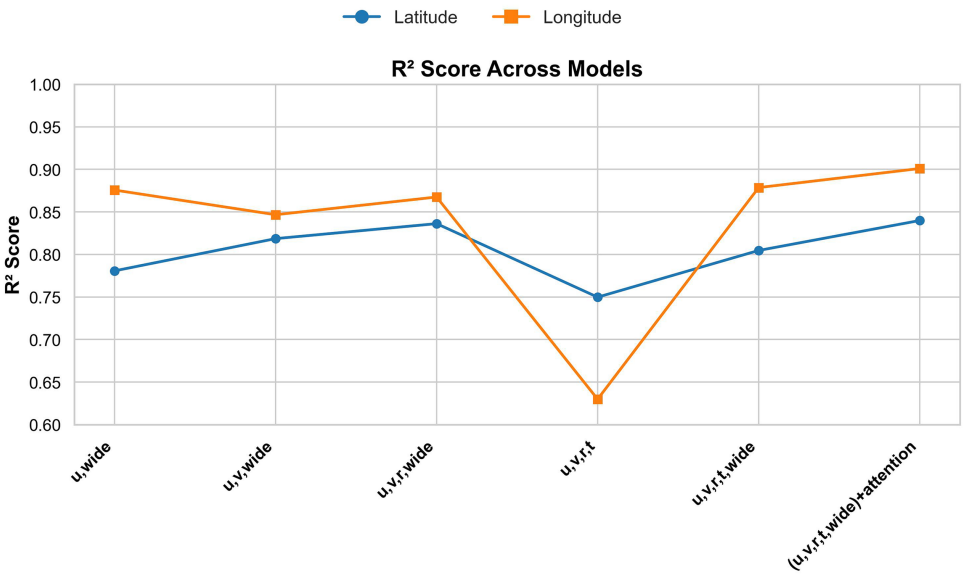

Figure 3: Performance visualization of the STAG-Net model for component-wise fusion.

The performance of the proposed STAG-Net model was assessed using two real-time cases of TC genesis: MINDULLE (2016) and YAGI (2013). In the case of TC MINDULLE, the actual genesis coordinates were (17.3°, 142.5°), compared to the predicted coordinates (17.88°, 142.09°). This results in a latitude MAE of 0.5826° and a longitude MAE of 0.4147°, which reveals significant model performance. Similarly, the actual coordinates of TC YAGI were (17.8°, 129.9°), and the predicted coordinates by STAG-Net were (17.38°, 130.68°), with a latitude and longitude difference of 0.4209° and 0.7813°, respectively.

These findings indicate that STAG-Net has a high ability to forecast TC genesis locations with sub-degree error in latitude and longitude, as shown in Fig. 4. Fig. 5 shows the distribution of prediction errors, demonstrating right-skewed behavior, with most predictions clustered around the median (3.91°) and mean (4.59°), and a small number of extreme cases exceeding 10°.

To further examine the temporal robustness of the proposed model, the time gap between the start of the disturbance and the time taken to reach TC genesis was divided into four slots, i.e., 0–24 h, 24–48 h, 48–72 h, and more than 72 h. As can be seen from Table 5, the accuracy of the prediction gradually declines as the time interval increases. The lowest mean MAE is shown in the first 24 h (3.91°), whereas errors are noticeably higher for events longer than 72 h (7.73°). This trend shows that disturbances in the early stage are more predictable; on the contrary, long-duration genesis cases are more variable and uncertain, and thus, prediction error and dispersion increase.

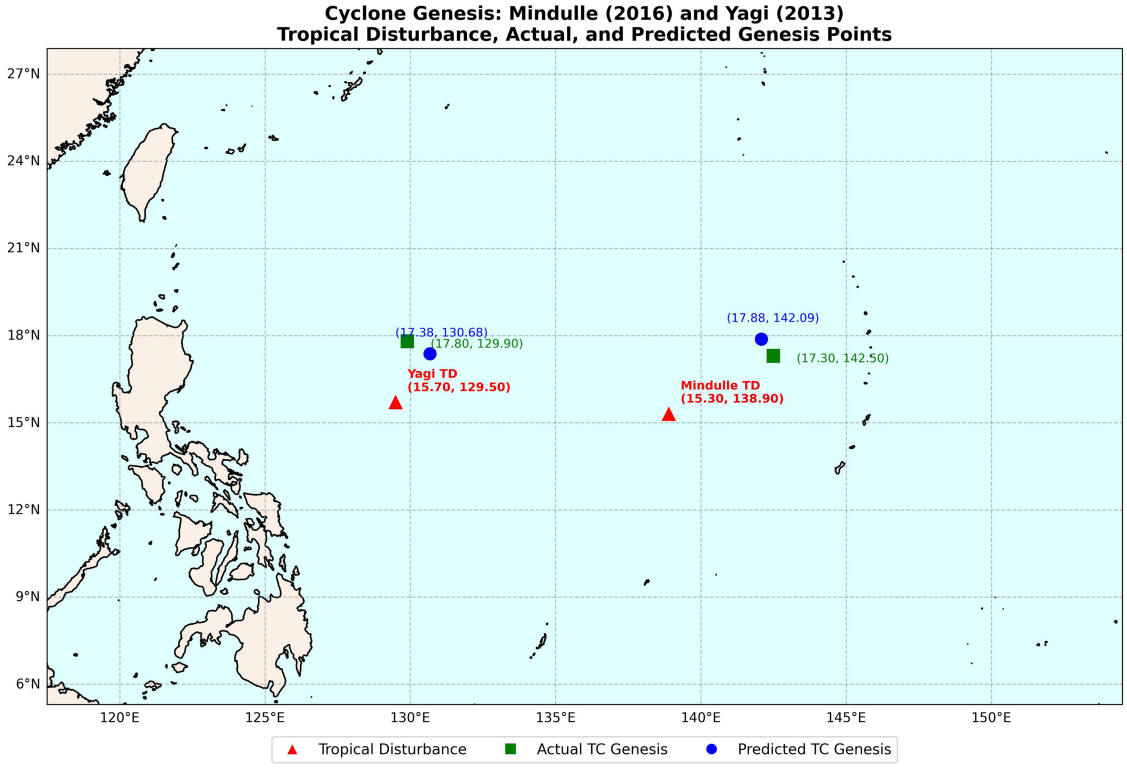

Figure 4: Performance visualization of the STAG-Net model on real-time TC MINDULLE (2016) and YAGI (2013) genesis locations.

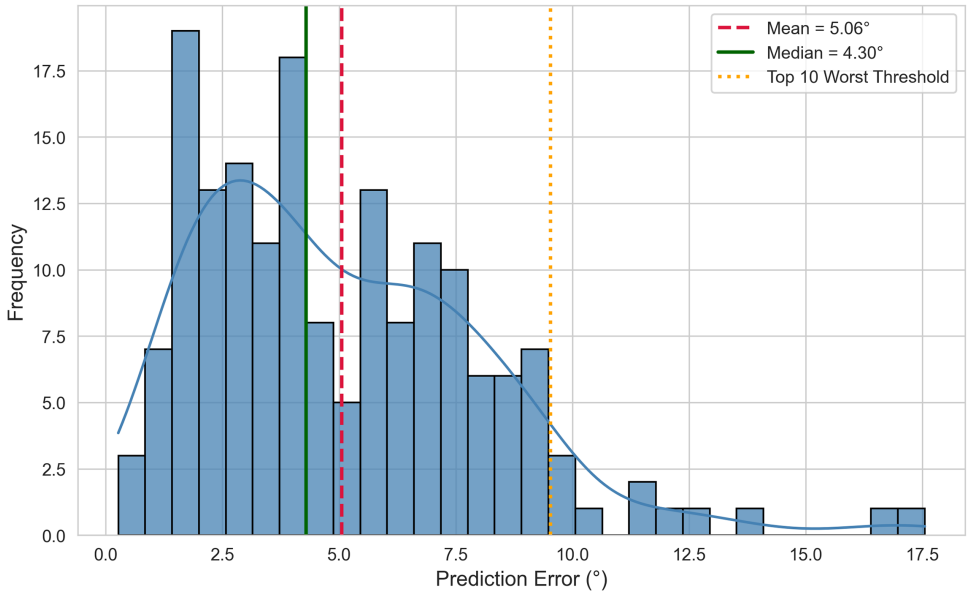

Figure 5: Distribution of tropical cyclone genesis location errors for test events.

Table 5: Time-slot-wise MAE analysis of TC genesis prediction performance.

Time Slot	Count	Mean MAE	Median MAE	Std. Dev.
0–24 h	24	3.9060	3.6468	1.7979
24–48 h	91	3.9731	3.4226	2.3033
48–72 h	35	4.8487	3.9736	3.6301
72 h+	20	7.7325	7.1940	5.1792

3.3.2 Performance of Attention Layer

To evaluate the effectiveness of the channel-wise attention layer, we compare the results of the STAG-Net model with ((u, v, r, t, wide) + attention) and without (u, v, r, t, wide) attention layer, as shown in Table 4. The results indicate that the baseline model obtained 1.9902° and 4.0082° MAE for latitude and longitude, and the channel-wise attention managed to improve the MAE to 1.7995° and 3.5567° for latitude and longitude, respectively. This shows a performance increase of up to 10% for latitude and 11.93% for longitude with respect to MAE. Furthermore, the model shows a performance increase of up to 19.85% and 20.25% for latitude and longitude, respectively, based on MSE.

The Gradient-weighted Class Activation Mapping (Grad-CAM) visualization, as shown in Fig. 6, highlights the spatial regions that are most important for predicting cyclone genesis for the TC named "Cecil." The activation map indicates an area of localized focus, which indicates that the model is perceiving physically meaningful structures in the atmosphere instead of diffuse structures.

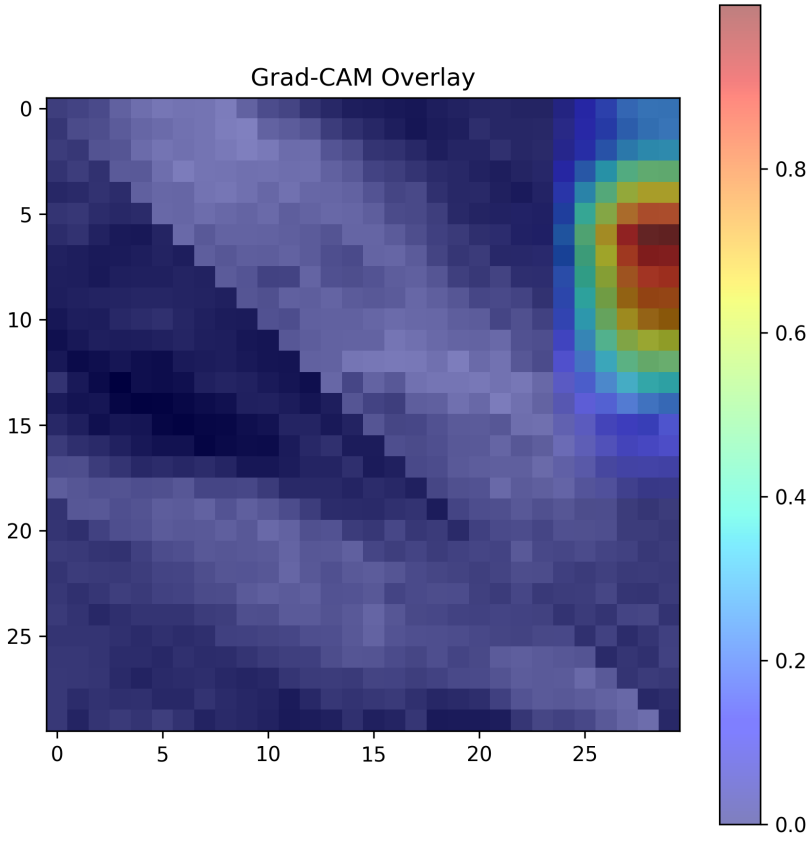

Figure 6: Grad-CAM overlay showing spatial importance regions for cyclone genesis prediction.

The great reason for this enhancement is that channel-wise attention enables the model to focus on the most useful feature maps at each convolutional block. In the prediction of the location of TC genesis, various meteorological factors (such as components of wind, temperature, relative humidity, etc.) play different roles at different locations. These feature channels are adaptively adjusted by the attention mechanism, which favours significant features and suppresses irrelevant or noisy ones. Such a selective focus is a part of more effective representation learning and therefore leads to less prediction error and better generalization.

3.3.3 Optimal Grid Size

To evaluate the impact of grid size in the proposed approach, we compare the performance of multiple grid sizes. In our experimental evaluation, we compare four different grid sizes (10×10, 20×20, 30×30, 40×40). These grid sizes are taken from smaller to larger to evaluate the impact on TC genesis location prediction. The results shown in Table 6 and Fig. 7 indicate that the grid size (30×30) achieves an average MAE of 2.67°, which is 7.54% lower than grid size (10×10), 6.55% lower than (20×20), and 2.5% lower than (40×40). Furthermore, the grid size (30×30) achieves an average R^2 score of 0.87, which is 4.8%, 3.75%, and 1.28% higher than the other three grid sizes, respectively.

Table 6: Grid size–wise performance comparison on latitude and longitude predictions.

Grid Size	Type	MAE	MSE	RMSE	R^2
10 × 10	Latitude	1.9243	7.4376	2.7272	0.7736
	Longitude	3.8518	24.5736	4.9572	0.8853
	Avg	2.88805	16.0056	3.8422	0.82945
20 × 20	Latitude	2.1038	7.2948	2.7009	0.7780
	Longitude	3.6152	21.6867	4.6569	0.8988
	Avg	2.8595	14.49075	3.6789	0.8384
30 × 30	Latitude	1.7995	5.2590	2.2932	0.8399
	Longitude	3.5566	21.2238	4.6069	0.9010
	Avg	2.67805	13.2414	3.45005	0.87045
40 × 40	Latitude	1.8427	5.7348	2.3947	0.8264
	Longitude	3.6489	22.1465	4.7060	0.8923
	Avg	2.7458	13.9407	3.5504	0.85935

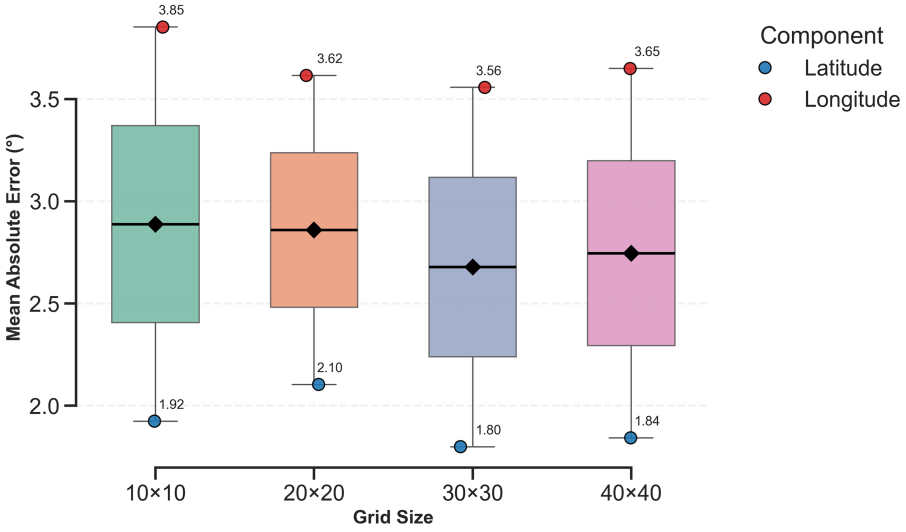

Figure 7: Performance visualization of grid size in the STAG-Net model.

The 30 × 30 attention grid offers a trade-off between spatial detail and stability, allowing meaningful areas of focus to be captured without injecting too much noise, as shown in Fig. 8. Such a tendency indicates that larger grids provide a more enriched spatio-temporal setting, with additional information about the surrounding atmospheric conditions of the disturbance being used. Consequently, this makes the model more competent in capturing the dynamics; thus, learning the spatial patterns that affect cyclone formation is improved.

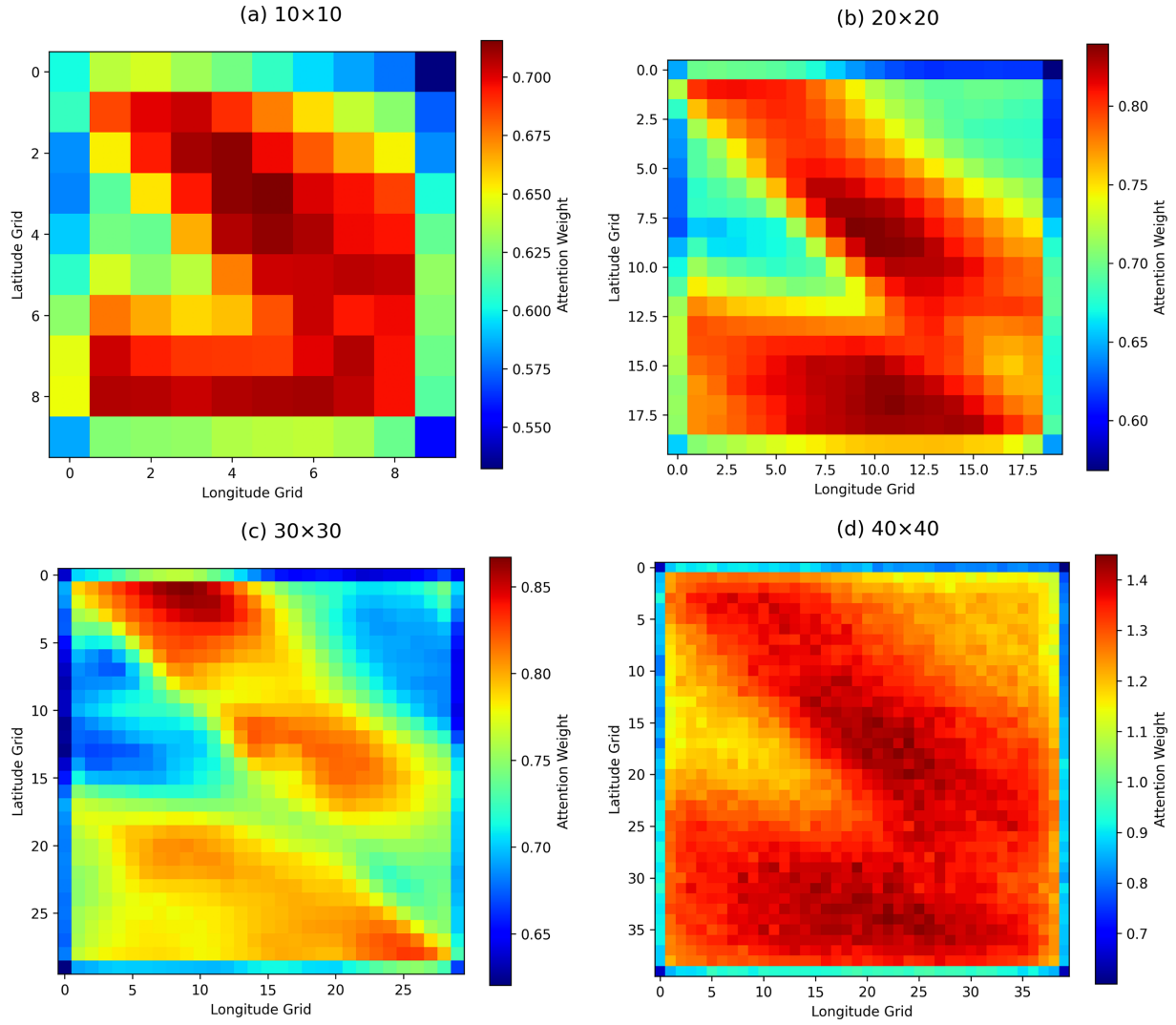

Figure 8: Channel-wise attention maps for all grid sizes illustrating the model's focus regions.

However, further increasing the grid size beyond 30 × 30 may not necessarily ensure further performance improvement. Extremely large grids could add non-informative or noisy environmental information from areas far away from the cyclone core dynamics, which could reduce the signal-to-noise ratio. Additionally, the computational complexity scales quadratically with the grid dimension, which could result in decreased accuracy relative to the increased training cost.

3.3.4 Comparison with Baseline Models

Most of the existing work on TC genesis prediction is presented in the context of a binary classification problem (i.e., genesis vs. non-genesis); therefore, these studies do not allow direct comparison with our coordinate prediction problem. Hence, we adjust the most suitable baseline models to fit our regression-based model in order to make a fair comparison.

We modified three baseline models: a temporal model (GRU) [36], Saf-Net [37], and the Dynamic Spatio-temporal model (DST) [16]. To ensure a fair comparison, only the last classification layers of the

baseline models were changed, while the original feature extraction architectures were kept unchanged. Specifically, the sigmoid/softmax output layers were replaced with fully connected linear layers having two outputs (latitude and longitude), and the binary cross-entropy loss was replaced with Mean Squared Error (MSE). All convolutional, attention, and recurrent modules remained unchanged to maintain architectural consistency.

The results shown in Table 7 and Fig. 9 provide a clear indication that STAG-Net efficiently outperforms the baseline models with regard to all important performance metrics, including MAE, MSE, RMSE, and R^2. The results indicate that STAG-Net achieved an average MAE of 2.678°, which is 9.75% lower than the DST model (which achieved the highest error among the baseline models). Furthermore, the proposed model achieved 26.25%, 12.95%, and 4.27% performance improvement with respect to MSE, RMSE, and R^2, respectively. This comparison shows that the combination of spatial and temporal interdependencies, along with attention mechanisms as in STAG-Net, provides a valuable contribution toward enhancing TC genesis location prediction.

Table 7: Performance comparison of STAG-Net with baseline models.

Model	Type	MAE	MSE	RMSE	R^2
GRU	Latitude	2.6753	10.3304	3.2141	0.6856
	Longitude	4.2233	30.1731	5.4930	0.8592
	Avg	3.4493	20.25175	4.35355	0.7724
Saf-Net	Latitude	2.0497	7.0671	2.6584	0.7849
	Longitude	3.9839	28.4618	5.3350	0.8672
	Avg	3.0168	17.76445	3.9967	0.82605
DST	Latitude	1.9045	6.6381	2.5765	0.7980
	Longitude	4.0006	27.8501	5.2773	0.8700
	Avg	2.95255	17.2441	3.9269	0.8340
STAG-Net	Latitude	1.7995	5.2590	2.2932	0.8399
	Longitude	3.5566	21.2238	4.6069	0.9010
	Avg	2.67805	13.2414	3.45005	0.87045
% increase (Avg)		9.75%	26.25%	12.92%	4.27%

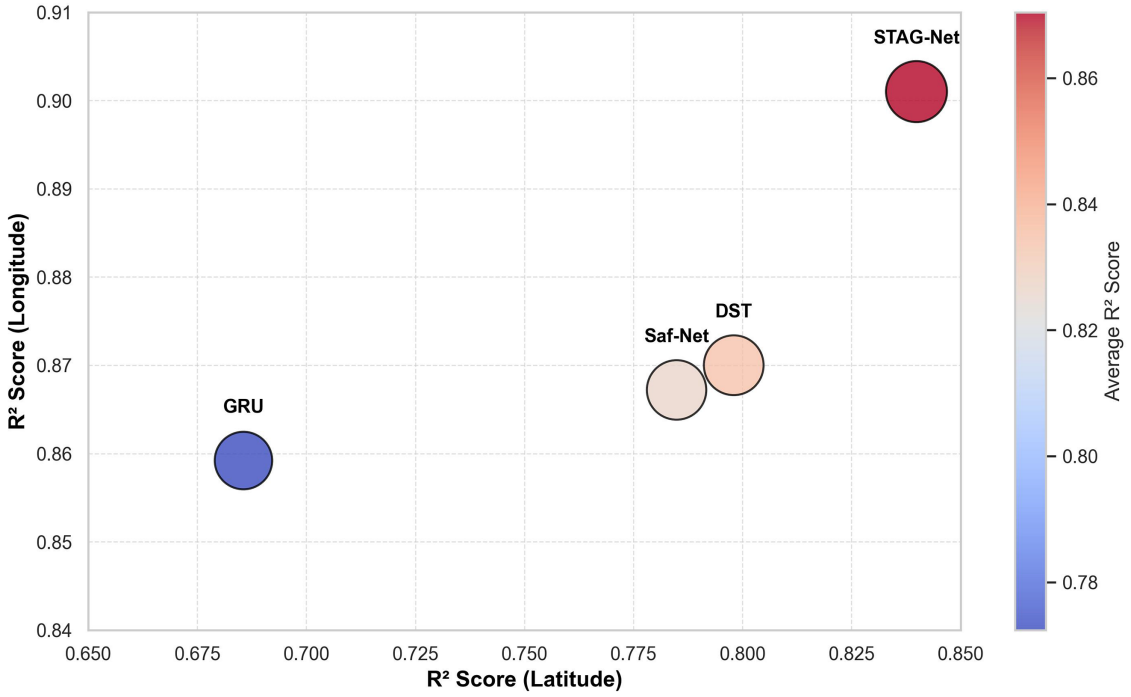

Figure 9: performance comparison of STAG-Net model with other temporal and Spatio-temporal models.

3.3.5 Discussion

The results of the study illustrate the efficiency of the proposed STAG-Net model for the prediction of TC genesis location. STAG-Net exceedingly performs better than the baseline temporal and spatio-temporal models in different evaluation metrics, namely MAE, MSE, RMSE, and R^2. Such increased performance can be explained by the ability of the model to simultaneously take into account the spatial and temporal patterns using u-wind, v-wind, relative humidity, temperature, and large-scale contextual information (wide). The combination of these different features allows the model to learn general representations of tropical disturbances and their evolution to cyclones.

The addition of channel-wise attention mechanisms is another reason why the model has achieved better performance. Such attention modules help the model to focus on the most relevant feature maps by giving it importance scores, in this way minimizing the influence of irrelevant or noisy data. Consequently, the model shows a better performance in capturing more informative and discriminative features, which is very beneficial for the generalization ability.

Besides, the grid resolution of 30 × 30 is also optimal and favorable with respect to the trade-off between spatial resolution and computational speed. It ensures that adequate environmental context is incorporated during training without introducing too much irrelevant information into the model. Moreover, the finding that the model successfully and consistently runs real-time cyclone case studies (e.g., Mindulle and Yagi) indicates strong quality and real-world applicability in an operational forecasting environment.

The proposed model processes a dense tensor but is nonetheless computationally feasible for early-warning applications. For the case of 30 × 30, as shown in Table 8, the total training time was 110.76 s, with an average training time per epoch of 0.87 s. The total inference time was 9.35 s, or 55.01 ms per sample. These results show that once trained, the model is able to make predictions in milliseconds, which meets

near-real-time operational needs. Training is performed offline, while inference speed is fast enough to be used in early-warning systems.

Table 8: Training and inference performance across different grid sizes.

Grid Size	Total Training Time (s)	Avg. Time/Epoch (s)	Total Inference Time (s)	Inference Per Sample (ms)
10×10	18.40	0.15	1.55	9.17
20×20	73.84	0.58	6.23	36.67
30×30	110.76	0.87	9.35	55.01
40×40	197.76	1.55	16.65	98.00

Although the proposed STAG-Net model shows positive results, there are several limitations. For example, the model is based on a fixed-grid resolution and does not dynamically adapt to different spatial scales of various tropical disturbances. Further, the model is likely to perform poorly in areas or seasons where past cyclone activity is limited due to insufficient training data. Addressing such issues in future work would improve the robustness and extensibility of the model.

Furthermore, the current work mainly focuses on multi-level atmospheric dynamics to study vertically structured predictors of cyclogenesis. While considering model dimensionality and computational cost, single-level thermodynamic spatial fields such as ocean heat content were not fully integrated into the spatial branch, which may limit the representation of oceanic energy contribution to genesis.

4 Conclusion

This study introduces STAG-Net, a novel Spatio-Temporal Attention-Gated Network, which combines multivariate meteorological inputs, i.e., u-wind, v-wind, relative humidity, temperature, and large-scale features, together with convolutional layers, GRU, and a channel-wise attention mechanism. The study utilized the initial tropical disturbance data to extract spatial information from the ERA5 reanalysis data store. The reanalysis data were extracted in the form of grids for 37 different isobaric planes and 4 different variables. Furthermore, the study also evaluates the impact of grid size and compares four different grid sizes $(10 \times 10, 20 \times 20, 30 \times 30, 40 \times 40)$ for TC genesis location prediction.

The performance obtained in the evaluation shows significant improvement compared with the benchmark DST model. Specifically, the Average Mean Absolute Error (MAE) decreased to 2.67°, the Mean Squared Error (MSE) to 13.24, RMSE to 3.45, and R^2 to 0.87045. This shows performance improvement of up to 9.75%, 26.25%, 12.92%, and 4.27% for average MAE, MSE, RMSE, and R^2, respectively. The results also indicate that the larger grid size (30×30) achieves higher performance compared to the other grid sizes.

Future investigations will be aimed at methodological extensions to make the models more robust and applicable in practice. To start with, the dynamic grid resolution will be implemented with the help of a multi-scale input strategy, and coarse and fine-resolution grids will be selected dynamically based on the level of disturbances and environmental variability. This can be hierarchical CNNs or attention-based spatial scaling. Second, multi-source data fusion will use feature fusion or learning of a transformer to combine the satellite brightness temperature data and radar precipitation fields. Third, uncertainty quantification will be integrated either through Monte Carlo dropout or ensemble learning to compute the prediction confidence intervals. Finally, real-time data ingestion pipelines will be developed for operational forecast applications.

Acknowledgement: This research is supported by Princess Nourah bint Abdulrahman University Researchers Supporting Project number (PNURSP2026R760), Princess Nourah bint Abdulrahman University, Riyadh, Saudi Arabia. The authors are thankful for the support of the Artificial Intelligence & Data Analytics Lab (AIDA), CCIS Prince Sultan University, Riyadh, Saudi Arabia.

Funding Statement: This research is supported by Princess Nourah bint Abdulrahman University Researchers Supporting Project number (PNURSP2026R760), Princess Nourah bint Abdulrahman University, Riyadh, Saudi Arabia.

Author Contributions: Kalim Sattar led the research and conducted the design and methodology. Malik Muhammad Saad Missen supervised the methodological development. Syeda Zoupash Zahra carried out the result analysis. Najia Saher and Rab Nawaz Bashir contributed to manuscript writing and content organization. Oumaima Saidani, Shahid Kamal and Muhammad I. Khan validated the methodology and results. All authors reviewed and approved the final version of the manuscript.

Availability of Data and Materials: GitHub repository: https://github.com/chkalim/TC_Genesis.

Ethics Approval: Not applicable.

Conflicts of Interest: The authors declare no conflicts of interest.

References

1. Hon KK, Ballard R, Blake E, Bond S, Gile R, Halperin D, et al. Recent advances in operational tropical cyclone genesis forecast. Tropical Cyclone Res Rev. 2023;12(4):323–40. doi:10.1016/j.tcrr.2023.12.001.
2. Hu L, Wen T, Shao Y, Wang Q, Fang W, Yang J, et al. Economic impacts of tropical cyclone-induced multiple hazards in China. Earths Future. 2023;11(9):e2023EF003622. doi:10.1029/2023ef003622.
3. Camargo S, Sobel AH, Barnston AG, Emanuel KA. Tropical cyclone genesis potential index in climate models. Tellus A Dyn Meteorol Oceanogr. 2007;59(4):428–43. doi:10.1111/j.1600-0870.2007.00238.x.
4. Kimura R. Numerical weather prediction. J Wind Eng Indust Aerod. 2002;90(12):1403–14. doi:10.1016/s0167-6105(02)00261-1.
5. Nicholls N. Cognitive illusions, heuristics, and climate prediction. Bull Am Meteorol Soc. 1999;80(7):1385–98. doi:10.1175/1520-0477(1999)080<1385:cihacp>2.0.co;2.
6. Cheung KKW. A review of ensemble forecasting techniques with a focus on tropical cyclone forecasting. Meteorol Appl. 2001;8(3):315–32. doi:10.1017/s1350482701003073.
7. Chen R, Zhang W, Wang X. Machine learning in tropical cyclone forecast modeling: a review. Atmosphere. 2020;11(7):676. doi:10.3390/atmos11070676.
8. Choi KS, Moon JY, Kim DW, Chu PS. Seasonal prediction of tropical cyclone genesis frequency over the western North Pacific using teleconnection patterns. Theor Appl Climatol. 2009;100(1–2):191–206. doi:10.1007/s00704-009-0182-1.
9. Lee CY, Tippett MK, Camargo SJ, Sobel AH. Probabilistic multiple linear regression modeling for tropical cyclone intensity. Mon Weather Rev. 2015;143(3):933–54.
10. Wang Y, Rao Y, Tan ZM, Schönemann D. A statistical analysis of the effects of vertical wind shear on tropical cyclone intensity change over the western North Pacific. Mon Weather Rev. 2015;143(9):3434–53. doi:10.1175/mwr-d-15-0049.1.
11. DeMaria M, Kaplan J. An updated statistical hurricane intensity prediction scheme (SHIPS) for the Atlantic and Eastern North Pacific basins. Weather Forecast. 1999;14(3):326–37. doi:10.1175/1520-0434(1999)014<0326:auship>2.0.co;2.
12. Loi CL, Wu CC, Liang YC. Prediction of tropical cyclogenesis based on machine learning methods and its SHAP interpretation. J Adv Model Earth Syst. 2024;16(3):e2023MS003637. doi:10.1029/2023ms003637.

13. Park MS, Kim M, Lee MI, Im J, Park S. Detection of tropical cyclone genesis via quantitative satellite ocean surface wind pattern and intensity analyses using decision trees. Remote Sens Environ. 2016;183:205–14. doi:10.1016/j.rse.2016.06.006.
14. Qian Q, Chen Y, Jia X, Ma H, Dong W. Basin dependencies of tropical cyclone genesis environment and possible future changes revealed by machine learning methods. iScience. 2025;28(2):111714. doi:10.1016/j.isci.2024.111714.
15. Mu B, Wang X, Yuan S, Chen Y, Wang G, Qin B, et al. A deep learning-based global tropical cyclogenesis prediction model and its interpretability analysis. Sci China Earth Sci. 2024;67(12):3671–95. doi:10.1007/s11430-023-1383-6.
16. Sattar K, Malik Muhammad Saad M, Saher N, Nawaz Bashir R, Zoupash Zahra S, Faheem M, et al. Tropical cyclone intensity prediction using spatio-temporal data fusion. IEEE Access. 2025;13:70095–104.
17. Dias J, Gehne M, Kiladis GN, Sakaeda N, Bechtold P, Haiden T. Equatorial waves and the skill of NCEP and ECMWF numerical weather prediction systems. Mon Weather Rev. 2018;146(6):1763–84. doi:10.1175/mwr-d-17-0362.1.
18. Navascués B, Calvo J, Morales G, Santos C, Callado A, Cansado A, et al. Long-term verification of HIRLAM and ECMWF forecasts over Southern Europe: history and perspectives of numerical weather prediction at AEMET. Atmos Res. 2013;125–126(3):20–33. doi:10.1016/j.atmosres.2013.01.010.
19. López Gómez J, Troncoso Pastoriza F, Fariña EA, Eguía Oller P, Granada Álvarez E. Use of a numerical weather prediction model as a meteorological source for the estimation of heating demand in building thermal simulations. Sustain Cities Soc. 2020;62(3):102403. doi:10.1016/j.scs.2020.102403.
20. Wijnands JS, Qian G, Kuleshov Y. Variable selection for tropical cyclogenesis predictive modeling. Mon Weather Rev. 2016;144(12):4605–19. doi:10.1175/mwr-d-16-0166.1.
21. Halperin DJ, Hart RE, Fuelberg HE, Cossuth JH. The development and evaluation of a statistical–dynamical tropical cyclone genesis guidance tool. Weather Forecast. 2017;32(1):27–46. doi:10.1175/waf-d-16-0072.1.
22. Sattar K, Zahra SZ, Faheem M, Missen MMS, Bashir RN, Abbas MZ. Stacked ensemble model for tropical cyclone path prediction. IEEE Access. 2023;11:69512–21. doi:10.1109/access.2023.3292907.
23. Zhang Z, Yang X, Shi L, Wang B, Du Z, Zhang F, et al. A neural network framework for fine-grained tropical cyclone intensity prediction. Knowl Based Syst. 2022;241:108195. doi:10.1016/j.knosys.2022.108195.
24. Zhang T, Lin W, Lin Y, Zhang M, Yu H, Cao K, et al. Prediction of tropical cyclone genesis from mesoscale convective systems using machine learning. Weather Forecast. 2019;34(4):1035–49. doi:10.1175/waf-d-18-0201.1.
25. Wei M, Fang G, Ge Y. Tropical cyclone genesis prediction based on support vector machine considering effects of multiple meteorological parameters. J Wind Eng Ind Aerodynamics. 2023;243(1):105591. doi:10.1016/j.jweia.2023.105591.
26. Qian Q, Jia X, Lin Y. Reduced tropical cyclone genesis in the future as predicted by a machine learning model. Earths Future. 2022;10(2):e2021EF002455. doi:10.1029/2021ef002455.
27. Zhao J, Zhan R, Wang Y, Jiang L, Huang X. A multiscale-model-based near-term prediction of tropical cyclone genesis frequency in the northern hemisphere. J Geophy Res: Atmosph. 2022;127(22):e2022JD037267. doi:10.1029/2022jd037267.
28. Chen R, Wang X, Zhang W, Zhu X, Li A, Yang C. A hybrid CNN-LSTM model for typhoon formation forecasting. GeoInformatica. 2019;23(3):375–96. doi:10.1007/s10707-019-00355-0.
29. Tong B, He Y, Hu G, Duan Z, Chan P. AI-aided simulation of tropical cyclone genesis under climate change. Glob Planet Change. 2025;251(1–2):104809. doi:10.1016/j.gloplacha.2025.104809.
30. Materia S, García LP, van Straaten C, Sungmin O, Mamalakis A, Cavicchia L, et al. Artificial intelligence for climate prediction of extremes: state of the art, challenges, and future perspectives. WIREs Clim Change. 2024;15(6):e914. doi:10.1002/wcc.914.
31. Dainelli F, Pérez-Aracil J, Ascenso G, Scoccimarro E, Giuliani M, Sanz SS, et al. XAI-GPI: an interpretable and adaptive machine learning genesis index for tropical cyclones. J Geophy Res: Mach Learn Computat. 2025;2(4):e2025JH000865. doi:10.1029/2025JH000865.
32. Zhang G, Rao M, Yuval J, Zhao M. Advancing seasonal prediction of tropical cyclone activity with a hybrid AI-physics climate model. Environ Res Lett. 2025;20(9):094031. doi:10.1088/1748-9326/adf864.

33. Ferrero MA, Azzalini D, Giuliani M, Castelletti A, Cerutti F, Amigoni F. Trustworthy inductive knowledge for tropical cyclones formation detection. Cham, Switzerland: Springer Nature; 2025. p. 69–81. doi:10.1007/978-3-031-89366-7_5.
34. Ying M, Zhang W, Yu H, Lu X, Feng J, Fan Y, et al. An overview of the China meteorological administration tropical cyclone database. J Atmos Ocean Technol. 2014;31(2):287–301. doi:10.1175/jtech-d-12-00119.1.
35. Hersbach H, Bell B, Berrisford P, Hirahara S, Horányi A, Muñoz-Sabater J, et al. The ERA5 global reanalysis. Quart J Royal Meteorol Soc. 2020;146(730):1999–2049. doi:10.1002/qj.4803.
36. Hafeez AB, Alonso E, Riaz A. DTC-TranGru: improving the performance of the next-DTC prediction model with transformer and GRU. In: Proceedings of the 39th ACM/SIGAPP Symposium on Applied Computing. New York, NY, USA: ACM; 2024. p. 927–34.
37. Xu G, Lin K, Li X, Ye Y. SAF-Net: a spatio-temporal deep learning method for typhoon intensity prediction. Pattern Recognit Lett. 2022;155:121–7.